J. Micromech. Microeng. **11** (2001) 504–508 PII: S0960-1317(01)20519-1

An optimized micromachined convective accelerometer with no proof mass

X B Luo[1], Y J Yang[2], F Zheng[2], Z X Li[1] and Z Y Guo[1]

[1] Department of Engineering Mechanics, Tsinghua University, Beijing 100084, People's Republic of China
[2] Hebei Semiconductor Research Institute, Shijiazhuang 050051, People's Republic of China

Received 5 January 2001, in final form 12 April 2001
Published 19 July 2001
Online at stacks.iop.org/JMM/11/504

Abstract
Miniaturization, low cost and high performance of accelerometers have been the topic of extensive research. A kind of convective micromachined accelerometer without proof mass is described in this paper. It consists of a microheater and two temperature sensors which measure the temperature difference between two sides of the microheater caused by the effect of acceleration on free convection. The optimization consideration is conducted before fabrication; some key factors, heater size and power, cavity size, distance between the heater and the sensor and the working medium, are considered. The test for the optimized device shows that the linearity error is smaller than 0.35% under tilt conditions of natural gravity and smaller than 2% under acceleration to 10 g ($g = 9.81$ m s^{-2}). A sensitivity of 600 μV g^{-1} is measured for operating power of 87 mW, the response frequency is about 75 Hz and the corresponding noise equivalent acceleration is approximately 1 mg Hz$^{-1/2}$ at 25 Hz. The dependence of the sensitivity on the heating power is a nearly linear function and the resolution increases with heating power increasing.

1. Introduction

Many kinds of micromachined accelerometers have been used in engineering applications, including the automobile industry, navigation systems, the military industry, robotics systems, consumer electronics and toys. However, high-performance micromachined accelerometers of smaller size and lower cost are still desirable [1].

So far, the common designs of micromachined accelerometers such as capacitive accelerometers [2], piezoresistive accelerometers [2, 3], piezoelectric accelerometers [4], electrical tunneling accelerometers [5] and thermal accelerometers [6] all involve a solid proof mass, which is allowed to move under accelerating conditions. The existence of the proof mass brings about some disadvantages. Firstly, the ability to resist shock declines; the overload range cannot be wide. Secondly, the fabrication is complex and not suitable to integrated circuit (IC) technologies, consequently the size cannot be very small and start-up costs cannot be reduced. Thirdly, the sensing of the motion of the proof mass suffers from various problems [7], for example capacitive sensing, the most common sensing method, suffers from electromagnetic interference and the influence of parasitic electrostatic force.

Recently, a novel concept and device structure for acceleration were developed by Dao *et al* [8]. The operation of the accelerometer is based on free convection of a tiny hot air bubble in an enclosed chamber. It does not require a solid proof mass and is compact, lightweight, inexpensive to manufacture and sensitive to small accelerations. Leung *et al* [9] reported the implementation of the device structure by bulk-silicon fabrication, the test under natural gravity demonstrated that its sensitivity could reach 0.6 mg. Milanovic *et al* [10] fabricated two kinds of the convective accelerometers, thermopile and thermistor types, in standard IC technology. By comparing them with those in [8, 9], they thought that their accelerometers exhibited some significant advantages, such as low cost, miniaturization, integration and good frequency response. However, both Leung *et al* [9] and Milanovic *et al* [10] mentioned that due to the complexity of free convection, the device structures and working conditions of their accelerometers still needed to be optimized so that higher performance can be achieved.

In this paper, a micromachined convective accelerometer is described, the implementation of the device with consideration of optimization by a bulk-silicon fabrication process is reported. The experimental measurements on the optimized device prove that the device has better linearity and higher sensitivity and a preferable frequency response than other reported convective accelerometers.

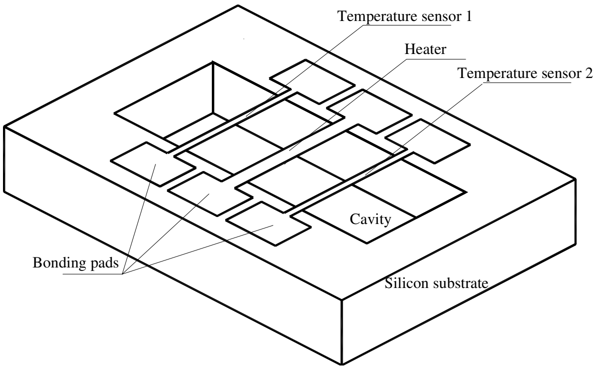

Figure 1. Device structure of the micromachined convective accelerometer.

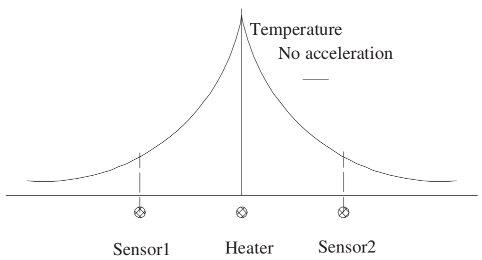

Figure 2. The symmetrical temperature profile under no acceleration.

2. Device structure and operation principle

Figure 1 shows the device structure of the micromachined convective accelerometer; it includes a cavity containing fluid, a heater for locally heating the fluid in the cavity and two temperature sensors positioned within a cavity such that the fluid moves across the sensors by virtue of free convection. The device is packaged in a sealed chamber to prevent air flow from disturbing the device's operation. When the heater is provided with a current, its temperature rises, then the fluid around it is heated, free convection is established in the cavity.

Figure 2 shows the temperature profile when the accelerometer is not subject to acceleration. In such a case, the flow pattern of the fluid is symmetrical about a vertical plane through the heat source. The temperature profile is also symmetrical, thereby, no temperature difference between two sensors is engendered. Figure 3 shows the temperature profile when the accelerometer is subject to acceleration. In such a case, the convection pattern is skewed so that the heat transfer to one temperature sensor increases and that to the other sensor decreases; thus a temperature difference is generated between the two sensors, which is proportional to the acceleration. By measuring the temperature difference, acceleration information can be acquired.

3. Optimization consideration

Since operation of the convective accelerometer is based on free convection, the key to upgrade its performance is to create suitable convection conditions in the device. Two non-dimensional parameters that decide the free convection pattern

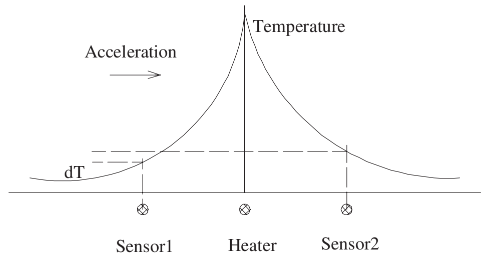

Figure 3. The distorted temperature profile by an applied acceleration.

in infinite space, the Grashof number Gr and the Prandtl number Pr, are introduced [11]:

$$Gr = \frac{a\beta\Delta T L^3}{v^2} \tag{1}$$

$$Pr = \frac{v}{\alpha} \tag{2}$$

where α, β, v and α are the acceleration, bulk expansion coefficient, kinematic viscosity and the thermal diffusivity, respectively; ΔT is the temperature difference between the heater and the environment; and L is the characteristic size, usually it denotes the heater width.

In order to make convective accelerometer work linearly, one should ensure that the temperature difference between the two sensors has a linear relation with the Grashof number, which also means that the temperature difference linearly relates to the acceleration from equation (1). Our numerical simulation for the convective accelerometer has shown that the temperature difference is linearly proportional to the Grashof number only under the condition that the Grashof number is larger than 10^{-4} and smaller than 10^3; beyond this range good linearity cannot be achieved. Thereby, to obtain good linearity it is necessary to control the Grashof number range for the convective accelerometer. According to equation (1), the corresponding design parameters must be selected to ensure the Grashof number range. All of the following discussion for increasing the sensitivity and response frequency should also be conducted on a precondition that the linearity of the convective accelerometer must be kept.

Since the temperature difference between the two sensors is linearly proportional to the Grashof number, it is obvious that a larger Grashof number will create higher sensitivity for the convective accelerometer at a given acceleration. So when needing high sensitivity, it is necessary to increase the Grashof number. Based on equation (1), the following measures can be taken to increase sensitivity:

(i) augmenting heating power, which means increasing ΔT;
(ii) increasing heater size, which means increasing L; this point shows a significant effect owing to the cubic relation of Gr with L;
(iii) choosing the working medium that has a small kinematic viscosity v.

The preceding discussion was aimed at free convection in an infinite space. For a confined space design in which the cavity height is comparable to the heater width, in addition to the Grashof number and the Prandtl number, the cavity

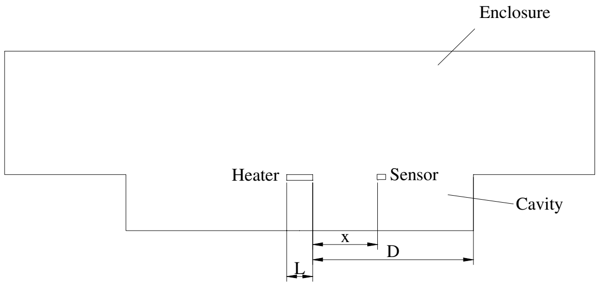

Figure 4. Simulation model of a convective accelerometer.

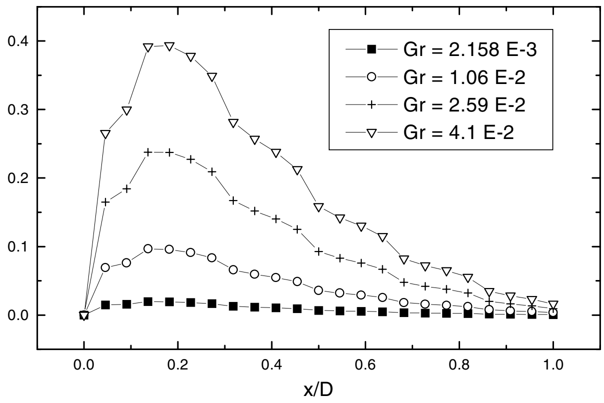

Figure 5. The variation of the temperature difference with the non-dimensional distance of the temperature sensor to the heater at different Gr.

boundary also affects the free convection. A small cavity size will restrain the flow by boundary action, which significantly affects the flow pattern in the convective accelerometer and makes the sensitivity drop. Thereby, increasing cavity size for small cavity design will increase the sensitivity.

Since the temperature sensor detects the temperature at a certain location of cavity, various temperature differences between two sensors will be created at different symmetrical positions; thereby, the position of temperature sensor is also an important factor for accelerometer performance. Numerical simulations are used to discuss this problem. Figure 4 shows the simulation model based on figure 1: x denotes the distance of the sensor to the heater, D denotes half of the size that the cavity width detracts the heater width. Figure 5 shows some results obtained by numerical simulation. The abscissa, x/D represents the non-dimensional distance of a temperature sensor to the heater, the ordinate represents the temperature difference between two sensors. It is noted from figure 5 that a temperature sensor has an optimum position for a large temperature difference at a given Gr, the position is near to the heater; thereby, properly choosing the distance between the heater and the temperature sensor will be advantageous for improving sensitivity.

As for the frequency response, it mainly depends on the thermal physical properties of the working medium; a large α and a small gas density ρ will hasten thermal diffusion, which correspondingly accelerates the heat uniformity in the accelerometer and a fast frequency response can be obtained. On the other hand, the frequency response also relates to the cavity size and the distance of the sensor to the heater. A large cavity size will make heat-balance time increase in the accelerometer at a fixed heater power, so the response frequency will drop. Otherwise, a small distance between the heater and the temperature sensor will make the response frequency increase. Based on the above discussion, it can be seen that improving the sensitivity and frequency response synchronously by changing cavity size is impossible, so when choosing the cavity size it is necessary to link the design with the accelerometer's application.

4. Fabrication

The device fabrication sequence is illustrated in figure 6. Starting with a ⟨100⟩ silicon substrate, a layer of silicon dioxide is formed using wet thermal oxidation, then a uniform layer of polysilicon is deposited in a LPCVD reactor and another layer of silicon dioxide is grown on it (figure 6(*a*)). The top oxide and polysilicon layers are patterned to make the heater, temperature sensor and polysilicon contact. After patterning, the polysilicon sidewalls are exposed (figure 6(*b*)). Then an oxide layer is produced on the polysilicon sidewalls by another oxidation step, which protects the polysilicon from anisotropic etching using ethylene diamine-pyrocatechol (EDP). On the oxide layer, the bonding pad and cavity windows are opened (figure 6(*c*)). A boron layer is then used to dope the silicon regions to make the electrical connections to the heater and sensors; afterwards, by patterned photolithography, a layer of Ti/Pt/Au metal is sputtered onto the top surface (figure 6(*d*)). When the metal is stripped, bonding pads and the cavity windows form (figure 6(*e*)). Finally, the wafer is wet-etched in EDP until the cavity is created (figure 6(*f*)). Figure 7 is a SEM photomicrograph of the device that is sealed in an enclosure.

5. Measurements

The accelerometer is measured under two kinds of application conditions. Firstly, it is tested from $-g$ to g under gravitation by rotating the sensitivity axis with respect to the Earth's gravitational field. Figure 8 illustrates the linearity of the accelerometer under gravitation. It shows a very good fit to the expected linear trend. The linearity error is smaller than 0.35%. For a comparison, the nonlinear coefficient of the accelerometer in [9] under gravitation is obviously larger than 1% at the 1 g point and that of the device in [10] is 0.5%.

The device is also measured on a vibration shaker within the acceleration range of 0 g to 10 g and frequency from 0 Hz to 200 Hz. Figure 9 shows that the device has good linearity in the range from 0 g to 10 g at 45 Hz. The linearity error is larger than that measured under gravitation, and reaches 2%. It is noted from figure 9 that the sensitivity of the optimized accelerometer is 600 μV g^{-1} for an operating power of 87 mW. For a comparison, the sensitivity of the accelerometer in [10] is 146 μV g^{-1} for the operating power of 430 mW, the linearity error in the acceleration range from 0 g to 7 g is 2%. Owing to the absence of relative comparable data, here the comparison with that in [9] cannot be carried out.

The frequency response of the device is shown in figure 10. It is noted that the frequency response is flat up to about 75 Hz, where the sensitivity decreases substantially. The response frequency is larger than that in [9], in which it is 20 Hz.

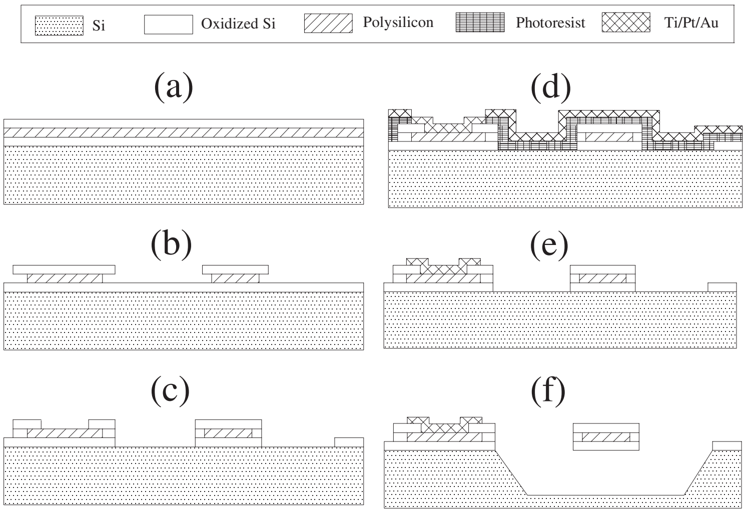

Figure 6. Device fabrication sequence.

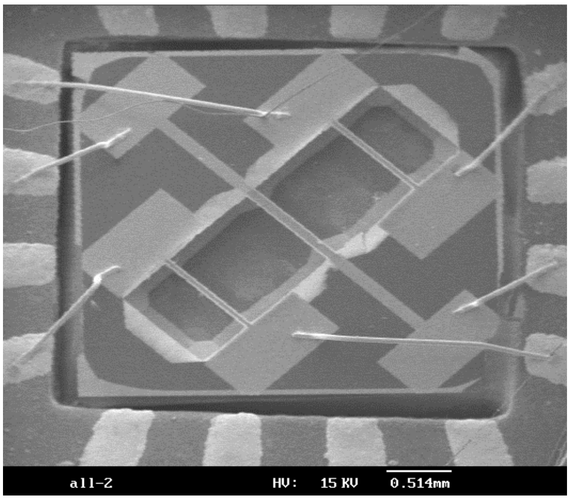

Figure 7. SEM photography of the device sealed in an enclosure.

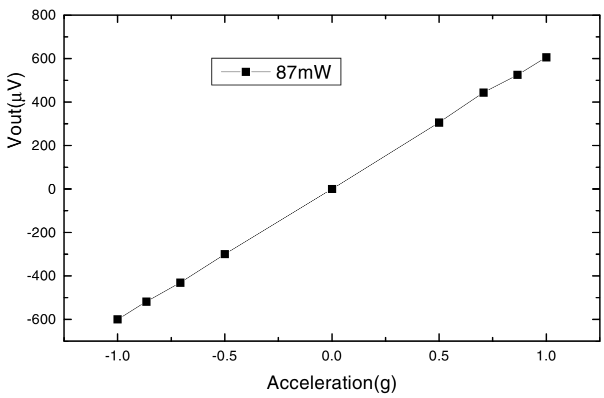

Figure 8. The linearity of the optimized accelerometer at 87 mW under gravitation.

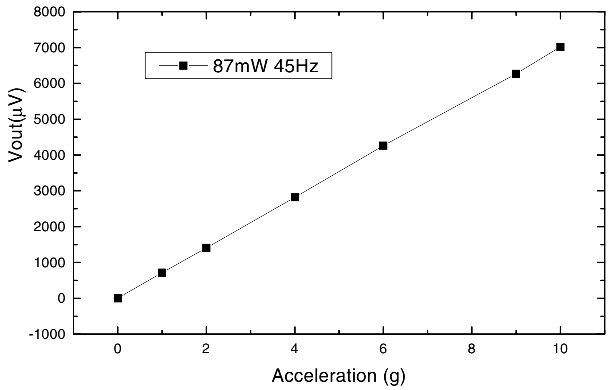

Figure 9. Measured performance of the accelerometer at 87 mW from 0 g to 10 g.

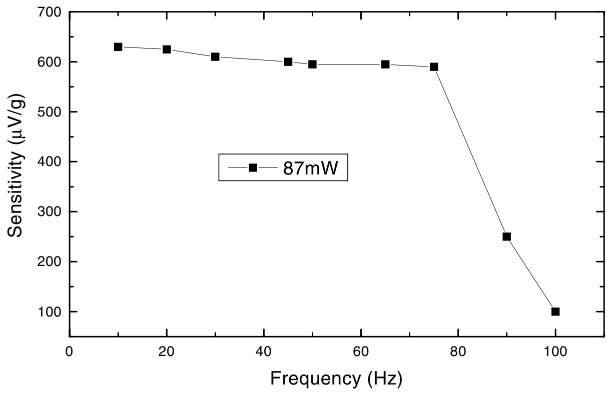

Figure 10. Measured frequency responses.

However, compared to the response frequency of 300 Hz in [10], it is much smaller. The main reason for this may be the fabrication method and the accelerometer size. In our present work, the same as that as in [9], traditional bulk-silicon fabrication is adopted, and the accelerometer size, including cavity size, are larger than that in [10], in which standard IC technology was employed. Based on the foregoing optimization analysis, the frequency characteristics of the present accelerometer cannot be as satisfactory as that in [10].

A noise test is also performed. The 25 Hz output noise at an operating power of 87 mW is 0.6 μV Hz$^{-1/2}$, so the

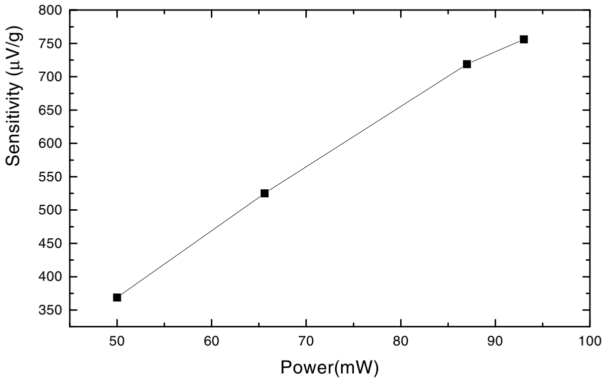

Figure 11. The variation of sensitivity with heater power.

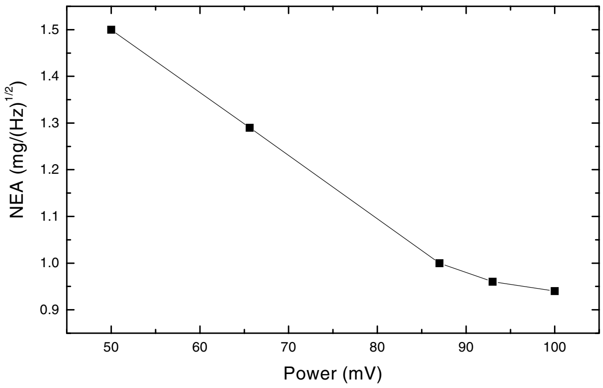

Figure 12. The variation of NEA with heater power.

noise equivalent acceleration (NEA) of the present convective accelerometer at 25 Hz is approximately 1 mg Hz$^{-1/2}$.

An investigation into the dependence of the sensitivity on the heating power was also conducted in the test under gravitation. Figure 11 shows that the sensitivity of the accelerometer is nearly linear with the heating power, proving that increasing the heating power can increase the sensitivity.

The variation of the NEA with the heating power at 25 Hz is demonstrated in figure 12. It is noted that the NEA of the convective accelerometer decreases with increasing heating power, which can be explained by the fact that when the heating power increases, the sensitivity increases linearly; however, the noise increases only slightly. So, the higher heating power will be favorable to gain better resolution.

6. Summary

A convective accelerometer without proof mass is described in this paper. A brief optimization analysis shows that the temperature sensor has an optimum position for high sensitivity, which is near the heater. An increase of the heating power, heater size and cavity size, under the condition that the accelerometer works linearly, leads to an increase in the sensitivity. However, increasing the cavity size also results in a decrease in the frequency response. The working media that has large thermal diffusivity α and small kinematic viscosity v will be favorable for fast frequency response and high sensitivity, respectively. Based on the optimization consideration, the optimized accelerometer is fabricated and tested. The result shows that it exhibits better linearity and higher sensitivity and has a preferable frequency response than some other reported convective accelerometers. The experiment also demonstrates that increasing the heating power will be advantageous in achieving good resolution.

Acknowledgments

This work was supported by the National Natural Science Foundation of China (grant No 59995550-2).

References

[1] Song Cimoo and Shinn Meenam 1998 Commercial vision of silicon-based inertial sensors *Sensors Actuators* A **66** 231–66

[2] Yazdi N, Ayazi F and Najafi K 1998 Micromachined inertial sensors *Proc. IEEE* **86** 1640–59

[3] Kim K H, Ko J S, Cho Y H, Lee K and Kwak B M 1995 A skew-symmetric cantilever accelerometer for automotive airbag applications *Sensors Actuators* A **50** 121–6

[4] Nemirovsky Y, Nemirovsky A, Muralt P and Setter N 1996 Design of a novel thin film piezoelectric accelerometer *Sensors Actuators* A **56** 239–49

[5] Kubena R L, Atkinson G M, Robinson W P and Stratton F P 1996 A new miniaturized surface micromachined tunneling accelerometer *IEEE Electron Device Lett.* **17** 306–8

[6] Dauderstadt U A, de Vries P H S, Hiratsuka R and Sarro P M 1995 Silicon accelerometer based on thermopiles *Sensors Actuators* A **46–47** 201–4

[7] Bochobza-Degani O, Seter D J, Socher E and Nemirovsky Y 2000 Comparative study of novel micromachined accelerometers employing MIDOS *Sensors Actuators* A **80** 91–9

[8] Dao R, Morgan D E, Kries H H and Bachelder D M 1996 Convective accelerometer and inclinometer *US Patent Specification* 5581034

[9] Leung A M, Jones J, Czyzewska E, Chen J and Pascal M 1997 Micromachined accelerometer with no proof mass *Technical Digest Int. Electron Device Meeting* pp 899–902

[10] Milanovic V *et al* 2000 Micromachined convective accelerometers in standard integrated circuits technology *Appl. Phys. Lett.* **76** 508–10

[11] Holman J P 1990 *Heat Transfer* 7th edn (New York: McGraw-Hill)